Multifractal analysis of complex signals

2007 Phys.-Usp. 50 819

(http://iopscience.iop.org/1063-7869/50/8/A03)

Physics – Uspekhi **50** (8) 819 – 834 (2007)

METHODOLOGICAL NOTES PACS numbers: **05.45. – a**, 05.45.Pq, 05.45.Tp

Multifractal analysis of complex signals

A N Pavlov, V S Anishchenko

DOI: 10.1070/PU2007v050n08ABEH006116

Contents

Abstract. This paper presents the foundations of the continuous wavelet-transform-based multifractal analysis theory and the information necessary for its practical application. It explains generalizations of a multifractal concept to irregular functions, better known as the method of wavelet transform modulus maxima; it investigates the benefits and limitations of this technique in the analysis of complex signals; and it discusses the efficiency of the multifractal formalism in the investigation of nonstationary processes and short signals. The paper also considers the effects of the loss of multifractality in the dynamics of various systems.

1. Introduction

The theory of fractals and multifractals [1 – 6] is currently widely used to describe self-similar and complex scaling properties observed in various physical systems [7 – 15]. Fractals are geometric objects (lines, surfaces, and bodies) that have a jagged shape and exhibit some degree of similarity (repetition) in a wide range of scales. The repetition can be complete (regular fractals) or might show some elements of randomness (random fractals). The structure of random fractals on a small scale is not identical to the structure of the entire object, but their statistical properties coincide and self-similarity persists after averaging over statistically independent realizations of the object.

A single quantity — the Hausdorff dimension or scaling exponent — is sufficient to statistically describe a fractal. It describes the preservation of both the geometry and the statistical properties under scaling. But many effects in physics, chemistry, biology, and other sciences exist that require generalizations of a fractal-like idea to more complex structures with additional scaling exponents. These structures are often characterized by a set of coefficients, and the Hausdorff dimension is just one of them [2, 3]. Complex fractals, called multifractals, are important because they most often occur in nature, while simple, self-similar objects only idealize real phenomena. In practice, the multifractal approach means that the object under study can be divided into parts each of which has its own self-similarity properties [2]. This approach, initially proposed for the statistical analysis of scaling properties of singular measures [16 – 20], has been successfully applied in diverse fields: in studying aggregation properties of blood cell elements in biology, in describing diffusive cluster growth and destruction of materials, in the theory of developed hydrodynamic turbulence, in investigating incommensurable structures and quasicrystals in solid state physics, in analyzing the RNA molecular structure, in the problems related to one-dimensional random walk and Brownian motion, and in describing invariant measures of strange attractors [21 – 26]. Multiple natural objects can be classified as 'multifractals,' and it would be very hard to find a branch of science that does not have representatives of this class.

Signals recorded in natural experiments are also important representatives of this class, and the existence of a precise mathematical approach to the analysis of complex structures of processes is undoubtedly valuable for a large number of practical problems. Simple or monofractal processes (for example, a $1/f$ noise or a Wiener random process) are homogeneous in the sense that their scaling parameters remain the same on any scale. The spectrum of such signals, $S(f) \sim f^{-\beta}$, does not change in a large frequency range, i.e., β is a constant. A multifractal process can be decomposed into regions with different local scaling properties [27]. Consequently, describing such a process requires a large

A N Pavlov, V S Anishchenko International Research Institute of Nonlinear Dynamics, Chernyshevskii Saratov State University, ul. Astrakhanskaya 83, 410026 Saratov, Russian Federation
Tel. (7-8452) 51 45 49, (7-8452) 51 57 38
E-mail: pavlov@chaos.ssu.runnet.ru, wadim@chaos.ssu.runnet.ru

Received 3 May 2006, revised 25 March 2007
Uspekhi Fizicheskikh Nauk **177** (8) 859 – 876 (2007)
Translated by L Zhukov; edited by A M Semikhatov

number of coefficients. In particular, the multifractal process spectrum cannot be described by a power law with a single exponent β.

Several known attempts to generalize the multifractal concept to functional signal dependences exist [27, 28]. One such attempt is based on the method of structure functions, which is often used in various fields of research. This approach is most popular in the study of strongly developed turbulence [27, 29]. In the early 1990s, Muzy, Bacry, and Arneodo [30, 31] proposed a more advanced method of the 'wavelet transform modulus maxima' (WTMM), which has significant advantages: the possibility of analyzing a wide range of singularities and their derivatives, smaller errors in computing the scaling characteristics, etc. The WTMM method has been successfully applied in studying the structure of inhomogeneous processes of various kinds. It is based on wavelet analysis [32 – 40], which is also called a mathematical microscope due to its ability to preserve good resolution on multiple scales.

We note that wavelet analysis is presently an extensive scientific field. Papers devoted to practical applications of the wavelet theory use the discrete form of the transform. This is because wavelet basis functions built on continuous wavelets are not strictly orthonormal. The discrete transform leads to a more accurate representation of a signal, in particular, in problems related to signal compression and reconstruction. It permits fast transforms and is important not only in information transmission but also in the analysis of random processes. Applying the discrete transform is more natural in the case of digitized data (time series) and is used in practice whenever it is required to quickly compute some characteristics. The continuous transform is slower, because it contains additional information. Nevertheless, there exist cases in the analysis of the structure of complex signals where such additional information can be helpful, allowing clearer results that are more intuitive to an expert with a basic radio-physical education. Moreover, these experts can more easily analyze the information presented by the continuous wavelet transforms, being able to visually follow the time behavior of instantaneous frequencies and amplitudes on different scales.

The WTMM method, which we consider below, was proposed by Muzy, Bacry, and Arneodo and is based on the continuous wavelet transform. This method is attractive because it allows considering both singular measures and singular functions and is much more universal in studying multi-scale properties of objects than the previously developed methods [27, 28]. Wavelets are often interpreted as a generalization of classical algorithms for covering a set by spheres, cubes, etc. Because the basis functions of the wavelet transform are well localized (soliton-like), they provide an effective mathematical method for analyzing nonstationary processes. Today, the WTMM method is one of the most popular methods to analyze nonstationary data.

After a publication on the multifractal description of cardiac rhythms in *Nature* in 1999 [43] and a subsequent series of papers [44 – 48], multifractal analysis became widely used as an instrument of applied studies and, in particular, of processing bio-medical measurements in the cases where the nonstationarity of the signals restricts using classical experimental data analysis methods. This method improves the chance of diagnosis based on wavelet theory, first demonstrated in [49], where the authors proposed a clinically important measure of heart beat irregularities. In the last several years, the multifractal structure has been discovered and numerically characterized in the dynamics of multiple systems of various natures. Some have said the WTMM method is one of the most effective methods to statistically describe inhomogeneous processes.

Because many processes in nature belong to the multifractal class, the multifractality property can be considered a very general rule of nature; this phenomenon merits study and description itself. Moreover, this study is practically valuable due to the possibility of developing new methods of analysis for experimental data based on the WTMM method and applicable to the solution of multiple problems. We note that few methods for processing nonstationary data exist. If the properties of a process change even in extremely short time intervals, then classical random process analysis algorithms can lead to errors in interpreting the results. The set of universal tools, applicable independently of stationarity, includes the interpretation based on the analytical signal concept [50, 51], the detrended fluctuation analysis [52, 53], and the wavelet analysis [32 – 40]. The multifractal method discussed in this paper is another instrument for this task. Although the WTMM method uses a wavelet analysis in intermediate calculations, it would be incorrect to regard this method as a part of wavelet analysis: it is a combination of two separate theories, the theory of wavelets and the theory of multifractals, which has profound similarities with statistical thermodynamics. Such a combination of two separate theories gives new opportunities to solve applied problems. Nevertheless, the WTMM method is not well known to applied scientists dealing with experimental data processing.

In this article, we describe the foundations of the theory of multifractal analysis of complex signals based on the continuous wavelet transform; we also provide the details needed for using the method in practice. The discussed method is quite difficult in application without a detailed methodology and a usage instruction. We try to provide such an instruction and make it simple and accessible to a broad audience. The examples of applications of the WTMM method are typically based on the authors' results. We paid special attention to describing new opportunities to analyze signal structure that are possible using this methods as well as to limitations and shortcoming of the multifractal formalism.

We show that multifractal analysis is an effective method of study of correlation properties of nonstationary random processes. We highlight the advantages of this approach compared to the classical correlation analysis for short-time signals.

2. Multifractal theory: from singular measures to singular functions

2.1 Fractal dimension

Fractal objects have self-similar properties and demonstrate various singularities (very irregular shape). Fractal dimension is traditionally used to numerically characterize the complexity of fractal geometry. Fractal dimension can be defined as follows. Let d be the dimension of a Euclidian space containing a fractal object. We cover this object with balls of diameter ε such that each point of the object is inside one of the balls. We assume that this takes at least $N(\varepsilon)$ balls. If, for a sufficiently small ε, $N(\varepsilon)$ satisfies the power law

$$N(\varepsilon) \sim \varepsilon^{-D_0}\,, \tag{1}$$

then D_0 is called the fractal dimension or fractal capacity of the object. The Hausdorff dimension D_H, which is also frequently used in the theory of fractals, is introduced as follows [54–56]. Let S be a set in R^n. We cover this set with balls with a diameter not exceeding ε. The Hausdorff measure l_δ is defined as

$$l_\delta = \lim_{\varepsilon \to 0} \inf_K \sum_i r_i^\delta , \tag{2}$$

where the inf operator determines the smallest value over all possible covers K of the set S by balls with diameter r_i ($r_i \leqslant \varepsilon$). This limit depends on the parameter δ. The Hausdorff dimension d_H is the value of δ at which l_δ is finite:

$$\begin{cases} \delta < d_H \Longrightarrow l_\delta = \infty , \\ \delta > d_H \Longrightarrow l_\delta = 0 . \end{cases} \tag{3}$$

According to this definition, d_H can take noninteger values.

Although the Hausdorff dimension is well defined from the mathematical standpoint, it is extremely hard to compute in practice. Consequently, many researchers prefer to work with more practical measures, such as the fractal capacity. For many fractals, D_0 and d_H coincide. In general, the inequality $d_H \leqslant D_0$ holds [57].

D_0 takes integer values for simple geometric objects such as a point, a straight line, or a smooth two-dimensional surface (corresponding to $D_0 = 0$, 1, 2) and noninteger values for self-similar fractal objects with a strongly irregular shape. One classical example is the Cantor set, whose construction procedure follows (Fig. 1). A unit-length segment is split into three equal parts and the middle part is removed. Then each of the two remaining parts is split into three parts and the middle one is removed. This process continues to infinity. The Cantor set is the infinite set of points that remain after this procedure. To compute the dimension of the Cantor set, we rewrite Eqn (1) as

$$D_0 = \lim_{\varepsilon \to 0} \frac{\ln N(\varepsilon)}{\ln (1/\varepsilon)} . \tag{4}$$

At the nth step of the construction, we have 2^n line segments of length $1/3^n$. As $N(\varepsilon)$ in this step, we can consider 2^n and take ε to be $1/3^n$. In the limit $\varepsilon \to 0$, which corresponds to the limit $n \to \infty$, we have

$$D_0 = \lim_{n \to \infty} \frac{\ln 2^n}{\ln 3^n} = \frac{\ln 2}{\ln 3} \approx 0.63 . \tag{5}$$

The Cantor set, like other regular fractals, preserves its geometry under scale changes in the range of ε where Eqn (1) holds. Rescaling leads to the power-law dependence $N(\lambda\varepsilon) = \lambda^{-D_0} N(\varepsilon)$.

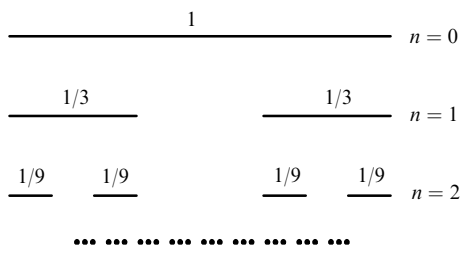

Figure 1. The Cantor set construction procedure.

2.2 Fractal measures

Fractals occur in nature not only as complex geometric objects. Various processes on fractals (physical, chemical, etc.) can generate stationary distributions called fractal measures. Examples of such measures include the invariant probability measure on a strange attractor, the distribution of growth probabilities in a process with limited diffusion aggregation, and the distribution of mass on a fractal set. While D_0 is used as a characteristic of the complex fractal geometry, the mathematical description of fractal measures involves a singularity spectrum $f(\alpha)$ [2]. This function has the following interpretation. We assume that there is a given measure distribution μ on a set, for example, a distribution of charge or mass. If this set is covered with balls of diameter ε, then the measure of a ball centered at a point x_i depends on ε in accordance with the power law

$$\mu_{x_i}(\varepsilon) \sim \varepsilon^{\alpha(x_i)}, \tag{6}$$

where $\alpha(x_i)$ is called the singularity exponent. Dependence (6) can be conveniently rewritten as

$$\alpha(x_i) = \lim_{\varepsilon \to 0} \frac{\ln \mu_{x_i}(\varepsilon)}{\ln \varepsilon} . \tag{7}$$

The smaller the value of $\alpha(x_i)$ is, the more singular the distribution of measure is at the given point. In the case of a uniform distribution, $\alpha(x_i) = 1$. The limit $\alpha(x_i) = 0$ corresponds to the measure distribution similar to the Dirac delta function, with the charge or mass concentrated at a single point [58]. The singularity spectrum $f(\alpha)$ characterizes the dependence on ε of the number of the covering elements N_α corresponding to the points with a singular exponent equal to some value of α:

$$N_\alpha(\varepsilon) \sim \varepsilon^{-f(\alpha)} . \tag{8}$$

By its meaning, f corresponds to the Hausdorff dimension [2]. In the case of a uniform measure distribution on a set, $\alpha = \text{const}$ and the singularity spectrum is a single point in the plane (α, f). In the case of a nonuniform measure distribution, the function $f(\alpha)$ has a more complicated bell-like shape.

Everything said can be illustrated with the Cantor set. We assume that it is endowed with a uniform distribution of measure μ, for example, mass, and 2^n elements (circles) with diameter $\varepsilon = 3^{-n}$ are used for the cover. The measure of each element in the cover is $\mu_{x_i}(\varepsilon) = 2^{-n}$, where x_i is the center of the circle. According to Eqn (7), the singularity exponent $\alpha(x_i)$ is determined by the slope of the dependence $\ln \mu_{x_i}(\varepsilon)(\ln \varepsilon)$, which takes the value $\alpha(x_i) = \ln 2/\ln 3$. In the limit $\varepsilon \to 0$, the value of the exponent corresponds to every point in the Cantor set. In the described example, the exponent α coincides with the Hausdorff dimension d_H and the singularity spectrum $f(\alpha)$ consists of a single point $f(\alpha) = \alpha \approx 0.63$ [2]. Thus, we observe only one type of singularity; such measures μ are called uniform [1, 3]

If the measure is nonuniformly distributed over the set, the singularity spectrum becomes more complicated. To illustrate this case, we consider the binomial distribution [2]. We assume that the segment [0, 1] is again partitioned into three parts, the middle one is discarded, but the two remaining parts [0, 1/3] and [2/3, 1] are assigned different weights p_1 and $p_2 = 1 - p_1 \neq p_1$. If at the beginning (at $n = 0$) we set $\mu_0 = 1$ for the entire interval [0, 1], then at the first step of the Cantor set construction, the two segments have the measures $\mu_1 = p_1\mu_0$ and $\mu_2 = (1 - p_1)\mu_0$. In the consecutive

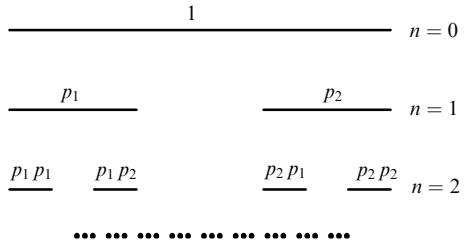

Figure 2. The Cantor set with a nonuniform distribution of measure.

steps, when splitting each segment into parts, we use the same weights p_1 and p_2 (Fig. 2).

After covering the fractal set with circles of radius $\varepsilon = 3^{-n}$, we consider the leftmost and rightmost elements of the cover. For the first one, containing the point $x_0 = 0$, the measure is $\mu_1 = p_1^n \mu_0 = p_1^n$. Then, according to Eqn (7), $\alpha(0) = \ln p_1 / \ln(1/3)$. Likewise, for the rightmost element of the cover, containing the point $x_0 = 1$, we can write $\alpha(1) = \ln p_2 / \ln(1/3)$. Because $p_1 \neq p_2$, $\alpha(0) \neq \alpha(1)$. Then the singularity spectrum no longer consists of a single point. The typical function shape in the case of a nonuniform measure is given in Fig. 3. The existence of a nonuniform distribution of measure on a set is a property of multifractal objects: the more nonuniform the measure is, the wider the spectrum of singularities is. We note that the maximum of $f(\alpha)$ coincides with the singularity spectrum in the case of a uniform distribution over the Cantor set, which characterizes the most common singularity.

In practice, it is difficult to compute the function $f(\alpha)$ using Eqn (8) because the convergence as $\varepsilon \to 0$ is very slow. Moreover, the values of the estimated characteristics can differ significantly for different points. Therefore, multifractal theory uses a special approach based on calculating generalized dimensions as global characteristics that can be used to compute the singularity spectrum $f(\alpha)$.

Within this approach, one introduces the generalized partition functions [58, 59]

$$Z(q, \varepsilon) = \sum_{i=1}^{N(\varepsilon)} \mu_i^q(\varepsilon) , \tag{9}$$

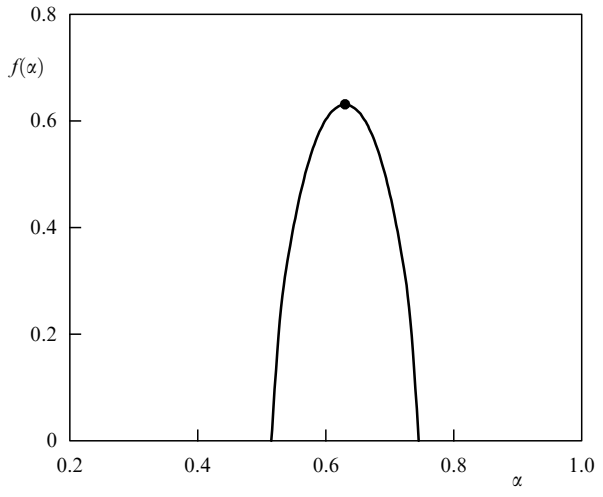

Figure 3. The singularity spectrum for a monofractal object (the Cantor set with a uniform measure distribution), the point; and a multifractal object (the Cantor set with a nonuniform measure distribution), the solid line.

where $N(\varepsilon)$ is the number of cover elements with size ε, μ_i is the measure of the ith element of the cover, and $q \in R$. The dependence of Z on ε typically obeys a power law:

$$Z(q, \varepsilon) \sim \varepsilon^{(q-1) D_q} , \tag{10}$$

where D_q are characteristics called the generalized fractal dimensions [60 – 63]. The coefficient $q - 1$ is introduced into the exponent to satisfy the normalization condition for μ, $Z(1, \varepsilon) = 1$. The combination

$$\tau(q) = (q - 1) D_q , \tag{11}$$

called the scaling exponent, is typically used. It follows from Eqn (9) and Eqn (10) that at $q = 0$, the equation reduces to the previously introduced definition of fractal dimension or capacity, Eqn (1).

For simple fractals, also called monofractals, $D_q = \text{const}$. In the general case of multifractal objects, the values of D_q monotonically decrease as q increases (Fig. 4a). This decrease can be considered a criterion confirming that the object is a nonuniform fractal. As a result, the dependence $\tau(q)$ is a straight line for uniform fractal measures and a nonlinear function for nonuniform measures (Fig. 4b).

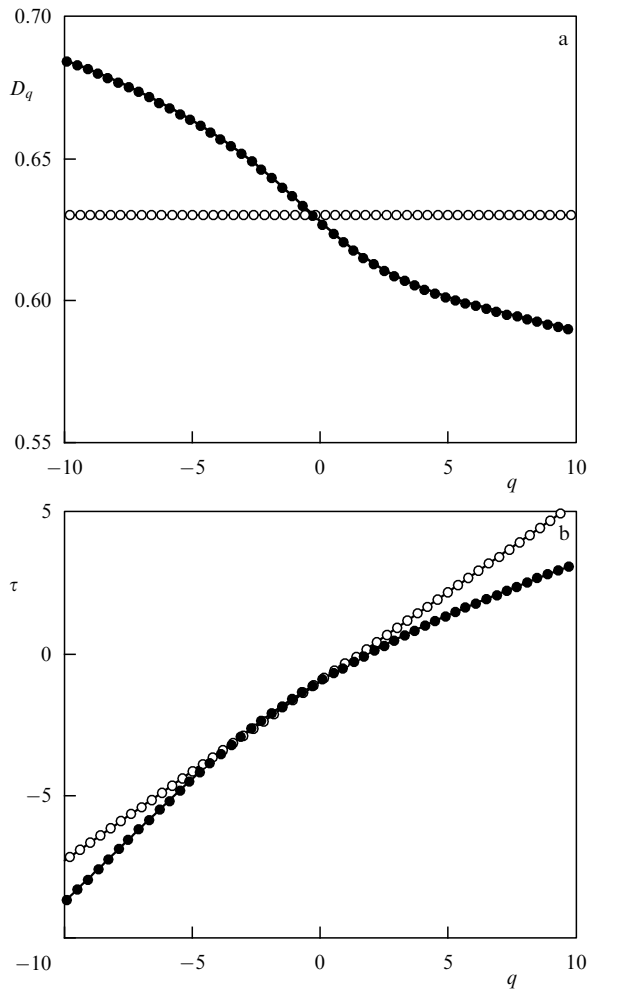

Figure 4. Spectra of the generalized fractal dimensions (a) and of scaling exponents (b) for a monofractal (white circles) and a multifractal (black circles).

The calculation of the singularity spectrum based on the scaling exponent $\tau(q)$ for the generalized fractal dimension is more stable and reliable than direct computations based on definition (8). Using this method, the functions $f(\alpha)$ are found via the Legendre transform:

$$\begin{cases} \alpha = \dfrac{\mathrm{d}\tau}{\mathrm{d}q}\,, \\ f(\alpha) = q\alpha - \tau(q)\,. \end{cases} \tag{12}$$

Thus, the sought function $f(\alpha)$ is immediately determined from the known spectrum of the scaling exponents $\tau(q)$. Multifractal analysis is often called the multifractal formalism, specifically referring to the approach where the singularity spectrum $f(\alpha)$ is regarded as a Legendre transform of $\tau(q)$. As pointed out in [64], a profound parallelism exists between the multifractal approach and statistical thermodynamics. The variables q and $\tau(q)$ play the same role as the inverse temperature and free energy; α and $f(\alpha)$ correspond to energy and entropy [17, 18, 65]. A number of rigorous mathematical results in the multifractal formalism have been obtained within the framework of dynamical system theory. In recent years, this approach is becoming increasingly popular in various experimental studies. We note, however, that the use of the term 'multifractal analysis' (although very widespread), might not always be correct, because the bell-shaped structure of $f(\alpha)$ in Fig. 3 can also be obtained for objects that are not multifractals. In the general case, there should be additional physical reasons to fully justify the use of the multifractal terminology. We mention limitations of the multifractal analysis in Section 5.

2.3 Fractal functions

The practical importance of multifractal theory would not be significant if it were only restricted to singular measures. But fractal objects occur in nature as singular functions, which suggests multifractal analysis as a tool for studying these complex signals; it is only necessary to adapt this tool for irregular processes.

The most intense research in random fractal functions may have been related to the study of diffusion processes or Brownian motion. In the one-dimensional case, the displacement of a Brownian particle $x(t)$ along a straight line is a random process with zero mean and dispersion

$$\langle x^2(t)\rangle \sim t\,, \tag{13}$$

where angular brackets denote averaging over the ensemble of realizations. The linear dependence of the dispersion on time in (13) characterizes the case of normal diffusion. The function $x(t)$ can be interpreted as a fractal [3] in the sense that its graph on a time–coordinate plot is a fractal point set with dimension $D_0 = 1.5$ (Fig. 5).

A more general case of Brownian motion is a fractal Brownian motion, where the displacement of a particle $x(t)$ in the one-dimensional space is a random process with the dispersion

$$\langle x^2(t)\rangle \sim t^{2H}\,, \tag{14}$$

where $0 < H < 1$. For $H \neq 0.5$, this dispersion corresponds to anomalous diffusion with correlated increments. The correlations of increments affect the graph of $x(t)$, making it more jagged ($H < 0.5$) or more smooth ($H > 0.5$). The

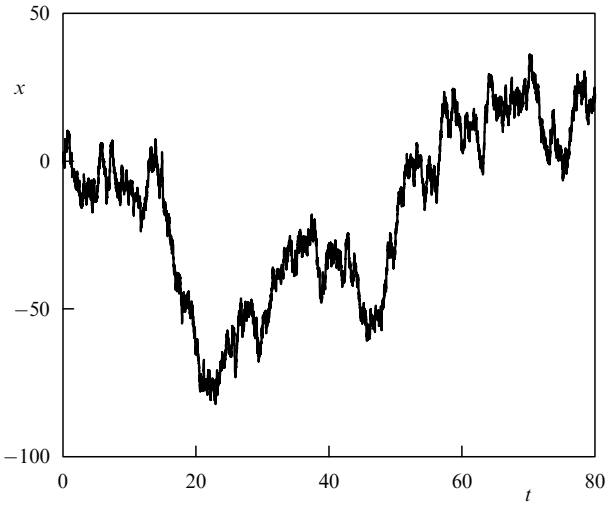

Figure 5. Brownian motion (the case of standard diffusion).

dimension, which is connected with the exponent H as [3]

$$D_0 = 2 - H\,, \tag{15}$$

In studying fractal functions, the dimension of the graph may be calculated, but this classical approach gives less information than the multifractal analysis, which allows obtaining a continuous spectrum of fractal dimensions and statistical data about the existence of various singularities. Computing a single quantity D_0 characterizes functions with only one type of singular behavior, which is constant in time (the case of a homogeneous fractal function). This is of course an idealization of real processes occurring in nature.

Brownian motion belongs to the class of random fractals: a scaled segment of $x(t)$ is not identical to the entire graph. Fractal theory often uses the notion of self-affinity to characterize sets that are invariant under affine transformations. In particular, in the plane, rescaling of a function graph with different magnification coefficients along the x and y axes leads to a graph that is similar to the original one. Self-similarity, which has been noted in relation to fractal objects, is, strictly speaking, a particular case of self-affinity and means similarity between an object and its segment scaled identically along both axes. For a self-affine function, we can write

$$g(x_0 + lx) - g(x_0) \simeq l^H\big(g(x_0 + x) - g(x_0)\big)\,. \tag{16}$$

In considering random processes like Brownian motion, an exact equality in Eqn (16) can be satisfied only for certain values of l and x_0. The exponent H in (16) is called the Hurst exponent [1, 4] and characterizes the irregularity degree of the function g at the point x_0. For $H < 1$, this function is non-differentiable and, in analogy to the previously introduced singularity exponent α, a smaller value of H corresponds to a stronger singularity in $g(x)$. The study of local irregular behavior of self-affine functions using multifractal analysis is a more informative approach compared to the study of the complex geometry of its graph on a time–coordinate plot. Because singularities of a function can be different at different points, they cannot be described with only a single parameter H in general. Therefore, by some modification of the definition of H, one introduces the notion of local Hurst

exponents, or Hölder exponents $h(x_0)$,

$$\left| g(x_0 + l) - g(x_0) \right| \sim l^{\,h(x_0)}, \tag{17}$$

which characterize the local singular behavior of g at the point x_0. As noted in [58], the multifractal approach to signal description characterizes a wide class of processes that are more complex than those that can be described by a single number (such as a single value of the fractal dimension or a single scaling parameter that corresponds, for example, to the frequency dependence of the spectral density).

The analysis of irregular functions, just as the analysis of fractal measures, is performed in terms of the singularity spectrum. But in considering functional dependences (irregular signals), the notation is changed. Instead of the spectrum $f(\alpha)$, one uses an analogous function $D(h)$; the Hölder exponent corresponds to α, and $D(h_0)$ is the dimension of the subset of the data characterized by the exponent h_0.

Several ways exist to compute the singularity spectrum. As in the case with fractal measures, computations based on its definition are hampered by the slow convergence and the fact that other singularities can occur even in the small neighborhood of x_0. The overlapping effect of several singularities leads to significant errors in calculating the scaling parameters and instability in numerical algorithms. To increase the confidence of $D(h)$ calculations, a statistical analysis is performed based on structure functions [27] or partition functions [30, 31]. The latter method is preferred, because it allows studying a wider range of singularities. In Section 3, we present the foundations of multifractal analysis with the computations of partial functions based on the wavelet transform.

3. Multifractal analysis based on the wavelet transform

3.1 Wavelet analysis of singular functions

At the beginning of the 1990s, Muzy, Bacry, and Arneodo proposed a novel approach for the study of multifractal signals of a complex structure — the method of wavelet transform modulus maxima [30, 31, 58]. This method, as follows from its name, is based on a wavelet transform that consists in a signal decomposition with respect to a basis built from a soliton-like wavelet function with certain properties using scaling transformations and translations. Each function in this basis represents a particular space or time frequency as well as its localization in physical space or in time [32 – 39].

The continuous wavelet transform of a function $g(x)$ is given by

$$W(a, b) = \frac{1}{\sqrt{a}} \int_{-\infty}^{\infty} g(x)\, \psi\left(\frac{x - b}{a} \right) \mathrm{d}x, \tag{18}$$

where a is a scaling parameter, b is a space or time coordinate, and ψ is a soliton-like wavelet function constructed, for example, using derivatives of the Gaussian function

$$\psi^{(m)} = (-1)^m \frac{\partial^m}{\partial x^m} \left[\exp\left(-\frac{x^2}{2} \right) \right]. \tag{19}$$

For a detailed description of the wavelet theory, we refer the reader to review [38]. For the study of local singularities of $g(x)$, the values $m = 1$ (a wave-wavelet) or $m = 2$ (an mhat wavelet) are typically used. Higher derivatives are used rarely. The choice of the basis function ψ is an important step in such a study: wavelets that reveal the desired information must be chosen. This can be done using various functions; continuing the analogy of wavelet analysis with a mathematical microscope, a choice of wavelet basis functions can be interpreted as a choice of microscope resolution: if the selected resolution reveals the desired details, then this wavelet is good for the problem. Moreover, selecting a lens (wavelet) with a higher resolution does not illuminate anything new.

As mentioned in Section 2.3, the degree of singularity of the g function can be described with the help of the Hölder exponent, whose mathematically more rigorous definition is as follows. We consider the case where a function g is n times differentiable at a point x_0, but the $(n + 1)$th derivative does not exist. Then $g(x)$ can be expanded into a Taylor series through the nth term. Let $P_n(x)$ denote the resulting polynomial of degree n. The Hölder exponent at the point x_0 is the maximal value of h for which the inequality

$$|g(x) - P_n(x - x_0)| \leqslant C\, |x - x_0|^h \tag{20}$$

holds. The higher the value of h is, the more regular (smooth) the function g is. Integration of the function increases the value of h by one and differentiation decreases it by one. We assume that the singular function under consideration can be represented as

$$g(x) = P_n(x) + C\, |x - x_0|^{h(x_0)}, \tag{21}$$

that is, as a sum of a regular component (a polynomial P_n) and the term that describes the irregular behavior and is characterized by a noninteger value of $h(x_0)$ [58]. One of the particularly widely used properties of the wavelet transform, used to remove the polynomial components of signals, is that the wavelets with the vanishing first m moments

$$\int_{-\infty}^{\infty} x^m \psi(x)\, \mathrm{d}x = 0 \tag{22}$$

are orthogonal to polynomials up to the degree m and

$$\int_{-\infty}^{\infty} P_n(x)\, \psi(x)\, \mathrm{d}x = 0 \tag{23}$$

for $m \geqslant n$. Therefore, the wavelet transform of $g(x)$ is

$$W(a, x_0) = C a^{1/2} \int_{-\infty}^{\infty} \psi(x) |\, ax\, |^{h(x_0)}\, \mathrm{d}x. \tag{24}$$

To simplify the analysis, it was proposed in [58] to slightly change the definition of the wavelet transform by multiplying the right-hand side of (18) by $1/\sqrt{a}$:

$$W(a, x_0) = \frac{1}{a} \int_{-\infty}^{\infty} \psi\left(\frac{x - x_0}{a} \right) g(x)\, \mathrm{d}x. \tag{25}$$

In this case, the simple power-law dependence

$$W(a, x_0) \sim a^{h(x_0)} \tag{26}$$

holds as $a \to 0$. Therefore, if a function $g(x)$ has a singularity at the point $x = x_0$, then its local singular behavior is characterized by the power law in (26). But if this function is

m-times continuously differentiable at x_0, then

$$W(a, x_0) \leqslant a^m \tag{27}$$

as $a \to 0$.

In the study of signal structure, one usually considers the function $g(x)$ itself, and rarely its derivatives. The signal is locally characterized by the dependence of the Hölder exponent on the signal point, and the values of the exponents are easily computed by the rate of decrease in the wavelet coefficients with the scale a. The faster the coefficients decrease as $a \to 0$, the more regular the function at that point is. Thus, the values of $W(a, x)$ in the vicinity of a point with a local singularity can diverge or decrease anomalously slowly. Such behavior of the wavelet coefficients allows a detailed analysis of the singularity structure.

3.2 The method of wavelet transform modulus maxima

The WTMM method studies irregular behavior of a function $g(x)$ in two stages. In the first stage, the wavelet transform is performed in accordance with Eqn (25). The result of the wavelet transform can be interpreted as a surface in a three-dimensional space (Fig 6a). The most important information is contained in the 'skeleton' — the lines of local extrema of the coefficient surface $W(a, x)$, which are sought at each a (Fig. 6b).

The choice of the basis functions is determined by the type of information to be extracted from $g(x)$. A necessary condition is that the selected wavelet have the smoothness not less than that of the signal. Regarding the choice of the parameter m in (19), we note that on one hand, increasing m allows ignoring large-scale polynomial contributions (that is, removing the trend) and analyzing small-scale variations of the function, but on the other hand, multiple differentiation leads to an increase in the number of lines of local extrema of the wavelet coefficients and to a large number of additional lines occurring at a small scale. Those lines are too short to conduct estimates of power dependences like (26) and become obstacles in a numerical study of the singularities. As pointed out in [36], the wavelet transform is constructed such that $W(a, x_0)$ is a regular function even if $g(x)$ is irregular. All the information about a possible singularity of $g(x)$, including its localization x_0 and exponent $h(x_0)$, is reflected in the asymptotic behavior of the coefficients $W(a, x_0)$ for small a. If the coefficients diverge at small scales, then g has a singularity at x_0 and the Hölder exponent can be found by plotting Eqn (26) in a double logarithmic scale and calculating the slope of $\ln W(a, x_0)(\ln a)$. If the coefficients $W(a, x_0)$ are close to zero in the vicinity of x_0 on a small scale, then g is regular at that point. An important observation in computing the Hölder exponent is that the sought characteristics are theoretically independent of the choice of the wavelet transform basis functions, which allows introducing a universal (in some sense) analysis of local irregularities [38] (although the wavelet representation, of course, depends on the chosen basis).

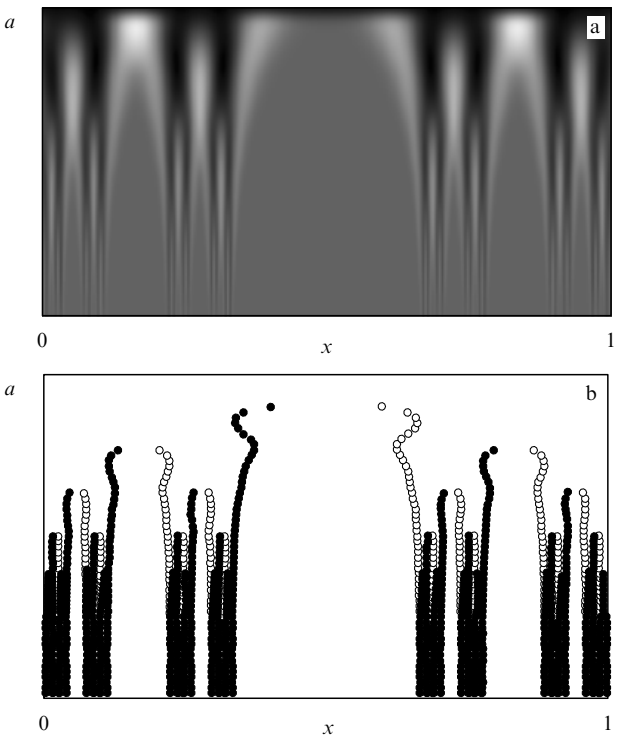

Figure 6. (a) A projection of a wavelet transform onto the ax plane. Larger values of the wavelet coefficients $W(a, x)$ correspond to darker regions. (b) Lines of the local extrema of the $W(a, x)$ coefficient surface; the minima are white circles and the maxima are black circles.

The first step of the WTMM algorithm concludes with the selection of a skeleton. The analysis of the selected lines of local extrema and the local maxima of the wavelet transform moduli theoretically allows computing the Hölder exponent, i.e. analyzing the singularities of $g(x)$. But this approach is only approximate; with an increase in scale, the influence of neighboring singularities increases, leading to various errors. In multifractal theory, it is preferable to perform calculations based on the so-called partition functions $Z(q, a)$ that allow obtaining more reliable estimates of the sought characteristics. Therefore, the second step of the WTMM method consists in constructing the partition functions as

$$Z(q, a) = \sum_{l \in L(a)} \left| W\left(a, x_l(a)\right) \right|^q , \tag{28}$$

where $L(a)$ is the set of all lines of local maxima of the wavelet-coefficient moduli that exist on scale a, and $x_l(a)$ characterizes the position of the maximum belonging to the line l. In this case, the use of the modulus of the wavelet coefficients ensures the stability of the method. Without that (using phase information), the method would not allow obtaining a stable solution. We note that in general, considering the maxima can lead to difficulties related to the stability of the method (it is better to operate with averaged values). Nevertheless, the wavelet transform procedure itself uses coefficients computed within a frequency – time window, which already provides averaging. Definition (28) does not work for negative q, because it is possible to have a situation where $W(a, x_l(a)) = 0$. In practice, therefore, another formula is used,

$$Z(q, a) = \sum_{l \in L(a)} \left(\sup_{a' \leqslant a} \left| W\left(a', x_l(a')\right) \right| \right)^q , \tag{29}$$

which means selecting the maximum value of the wavelet-coefficient modulus along each line on scales less than the given value of a. According to [30, 31], the relation

$$Z(q, a) \sim a^{\tau(q)} \tag{30}$$

holds, where $\tau(q)$, to be determined for some q from the slope of $\ln Z(q,a)(\ln a)$, is called the scaling exponent. Varying the powers q in constructing partition functions (29) yields a linear dependence $\tau(q)$ for monofractal objects ($H = \mathrm{d}\tau/\mathrm{d}q = \text{const}$) and a nonlinear dependence $\tau(q) = qh - D(h)$ with a large number of Hölder exponents $h(q) = \mathrm{d}\tau/\mathrm{d}q \neq \text{const}$ in the case of multifractals.

For some values of q, the scaling exponents $\tau(q)$ have a simple interpretation [58]. Thus, there is a dependence between $\tau(2)$ and the exponent β in the spectral power density function $S(f) \sim 1/f^{\beta}$:

$$\beta = 2 + \tau(2)\,. \tag{31}$$

Furthermore, because the spectral density function is related to the correlation function by the Fourier transformation, the known β allow determining the rate of decrease of correlations $\Psi(\tau) \sim \tau^{-\gamma}$, i.e., the exponent γ. The dependence between the basic quantities used within the WTMM method is determined by the Legendre transform

$$\begin{cases} h = \dfrac{\mathrm{d}\tau}{\mathrm{d}q}\,, \\ D(h) = qh - \tau(q)\,. \end{cases} \tag{32}$$

Compared to the method of structure functions, the multifractal analysis based on the wavelet transform allows investigating singularities at negative q. The partition functions $Z(q,a)$ for $q < 0$ characterize the scaling properties for weak singularities (small fluctuations), and for $q > 0$, for strong singularities (large fluctuations).

We illustrate the application of the WTMM algorithm with the example from Section 2, the Cantor set. To perform numerical computations, we construct a correspondence between the Cantor set and a binary sequence consisting of zeros and ones (zeroes correspond to deleted segments). Thus, at the beginning ($n = 0$), this sequence consists of one element (1), after the first step, three elements (101), after the second step, nine elements (101000101), and so on. As the fractal function $g(x)$, we take the distribution function of a uniform measure μ on the Cantor set. Normalizing the measure $\bigl(\mu([0,1]) = 1\bigr)$, we define $g(x)$ as

$$g(x) = \mu\bigl([0,x]\bigr) = \int_0^x \mathrm{d}\mu\,. \tag{33}$$

The resulting function is shown in Fig. 7. Selecting a $\psi^{(m)}$ mhat wavelet for the basis function and following the algorithm in Section 3.1, we first perform a wavelet transform of $g(x)$ and select lines of local maxima of the wavelet coefficient moduli. As can be seen from Fig. 6, the number of local maxima decreases with an increase in the scale a. According to Eqn (26), the local singular behavior of $g(x)$ can be analyzed by constructing the dependence of $\ln W(a,x_0)$ on $\ln a$ and calculating the slope of the fitting line. The results of calculations for various lines of local maxima are shown in Fig. 8a. Along with the expected values $h = \ln 2/\ln 3$, we find the Hölder exponent changing in a large range for short lines. The situation changes if we exclude lines disappearing at small scales and consider the power-law dependences of the wavelet coefficients, e.g., with $\ln a > 1.5$ (Fig. 8b). To avoid difficulties related to poor small-scale resolution, we study scaling singularities at the scaling factors a that are not too small.

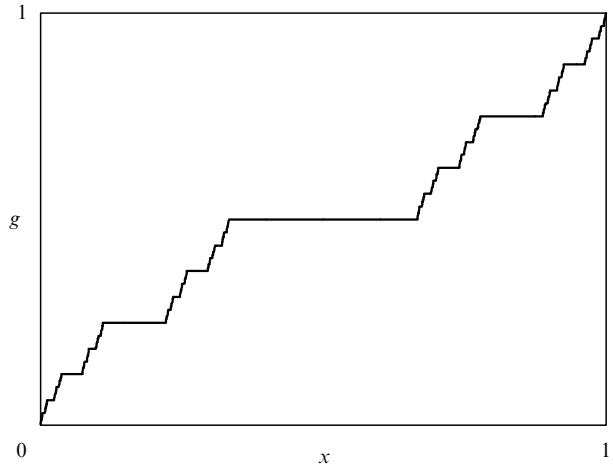

Figure 7. The uniform measure distribution function on the Cantor set.

Direct estimates of the Hölder exponent h from the power dependence of the wavelet coefficients are less accurate than the results for the spectrum $\tau(q)$ of partition functions and the calculation of the local slopes $h = \mathrm{d}\tau/\mathrm{d}q$ (the second step of

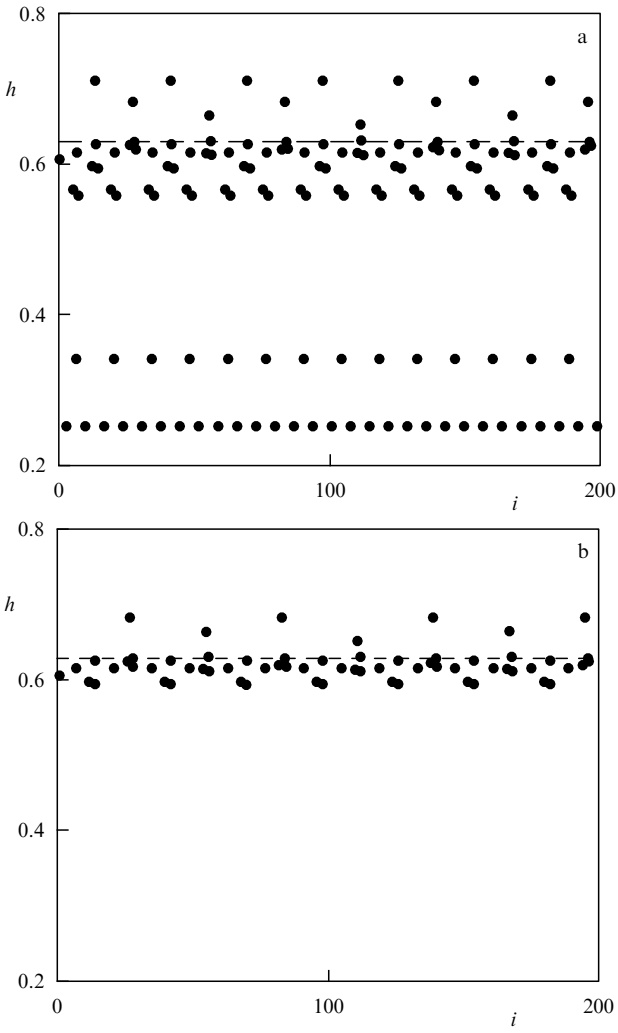

Figure 8. Hölder exponent values computed using the slope of the power-law dependence of form (26), for all lines of local extrema (a); without considering lines that terminate at small scales ($\ln a < 1.5$) (b).

the WTMM method). With a large number of steps n in the Cantor set construction, the numerically computed values of $h = d\tau/dq$ and the singular spectrum $D(h)$ almost coincide with theoretical results. For example, in calculations for $n = 10$, the deviation from the theoretical value $\ln 2/\ln 3$ does not exceed 1%.

We already noted that in the analysis of the local regularity of the signal based on the wavelet transform coefficients, the computed Hölder exponents are theoretically independent of the choice of the basis. In practice, however, such dependences do appear. In the majority of papers known to us, the wave and mhat functions (the first and second derivatives of a Gaussian function) were used as the basis functions. If higher-order derivatives are used as the analyzing wavelet, then the number of additional short lines of local maxima of $W(a, x_0)$ increases due to the oscillating tails of soliton-like functions $\psi^{(m)}$. In this case, a compromise is to be sought between ignoring polynomial components (the trend), which requires an increase in m, and a significant consequent increase in the number of short local maxima lines, which complicates the skeleton and leads to deviations from the power-law dependence at small scales. In practice, it makes sense to restrict m to small values (usually $m \leqslant 2$).

So far, we have considered the case of a uniform distribution of measure μ over a fractal set. Numerical analysis allows studying a more complicated example, the Cantor set with a random distribution of measure. In constructing such a set, the weights p_1 and $p_2 = 1 - p_1$ are taken to be $0.5 \pm \xi$ at each step, where ξ is a random variable. For the random variable with small dispersion, the structure of the resulting set is close to monofractal. With an increase in dispersion, the dynamics become multifractal: a point in the plane $D(h)$ is transformed into a bell-like dependence, typical of multifractals (Fig. 9). Thus, with a random distribution of measure on the Cantor set, the most probable singular measures correspond to the value $\ln 2/\ln 3$, and the multifractal degree, or the width of the spectrum $D(h)$ depends on the dispersion of the random variable ξ, i.e., the nonuniformity of measure distribution.

The multifractal analysis can be applied to signals of various natures. In addition to irregular realizations of continuous random processes, the WTMM method can be used, e.g., to analyze symbol sequences, like nucleotide chains in RNA. For this, they are represented as binary sequences $u(i) = 1$ or $u(i) = 0$ depending on the nucleotide labeled by i. Then, as in one-dimensional random-walk problems [52], one considers the sum

$$g(k) = \sum_{i=1}^{k} u(i)\,. \tag{34}$$

The correlation analysis of $g(k)$ using the WTMM method allows speaking of the absence of correlations in the symbol sequence if $h = 0.5$ and their presence if $h \neq 0.5$. Sometimes, correlations ($h > 0.5$) and anticorrelations ($h < 0.5$) are considered [52]. The dynamics of a binary sequence are anticorrelated when the probability of alternating pairs 01 or 10 is higher than the probability of the pairs 00 or 11. In the case of correlated dynamics, zeros are more often followed by zeros, and ones by ones, i.e., the probability of finding the 00 and 11 pairs increases. For continuous random processes, the Hölder exponents also allow detecting anticorrelated ($h < 0.5$) or correlated ($h > 0.5$) dynamics. In the first case, the alternation of large and small values in a random process is observed (a large value is followed by a small one with high probability, and vice versa). In the second case, a large value is more often followed by a large value, and a small by a small one; the process is smoother. The case of $h = 1$ corresponds to the $1/f$ noise, and $h = 1.5$ to the Wiener random process.

We note that the analysis of multiscale properties for sequences of form (34) leads to the same results as taking the g function to be the initial binary sequence $g(i) = u(i)$ if the $1/a$ prefactor is removed from (25). This is because integration increases h by 1. Taking this circumstance into account in Eqn (26), we can perform calculations without computing the sums in Eqn (34), which is equivalent to integrating with a variable upper limit. This property is useful in practical applications of the multifractal analysis method.

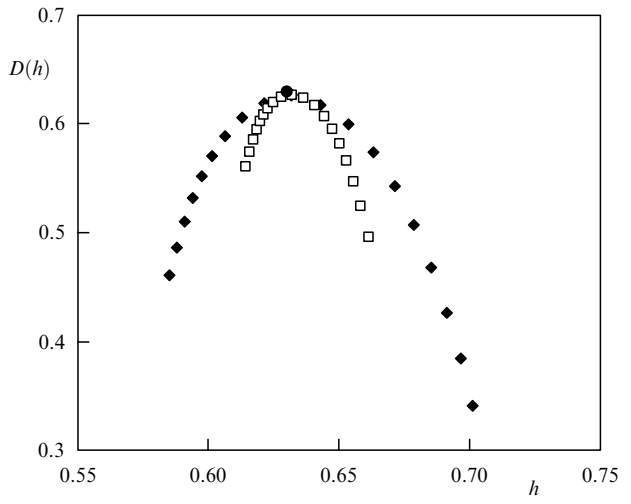

Figure 9. Singularity spectra for the Cantor set with a random distribution of measure. In creasing the spectrum width $D(h)$ corresponds to an increase in nonuniformity in the measure distribution.

4. Examples of multifractal analysis applications: the effects of losing multifractality

We consider several examples of applying the WTMM method to practical problems, which include testing the method for a quantitative description of known phenomena in nonlinear system dynamics (chaotic and stochastic synchronization), and also using multifractal analysis to diagnose the state of living objects from nonstationary signals. The examples were selected, on one hand, to demonstrate the universality of the method and on the other hand, to show the existence of common effects that allow using the degree of multifractality as a quantitative characteristic of the studied system state. We note that using the multifractal method based on wavelet analysis reveals more subtle characteristics compared to traditional methods of signal processing (for example, correlation analysis). The WTMM method is sensitive to the dynamics on various scales, from weak singularities (small fluctuations) to strong singularities (large fluctuations). The underlying wavelet transform is well suited for the study of self-similarity (in terms of wavelet coefficients, this means a power-law behavior of their higher moments with variations in scale). The method is well suited to the solution of physical problems, because it operates with characteristics intuitive to physicists. In particular, the singularity spectrum contains information about correlation properties of the studied processes as well as information

about the signal uniformity, quantitatively measured by the width of the $D(h)$ function.

4.1 Chaotic dynamics of interacting systems

As a first example, we consider testing the multifractal analysis for diagnosing the well-known chaos synchronization effect in the dynamics of interacting systems that produce self-sustained oscillations. The synchronization of chaotic oscillations leads to changes in the complex geometry of attractors compared to the noninteracting case. These changes are reflected in the structure of time intervals, such as the recurrence time to the Poincaré secant. According to [66], the distribution of recurrence times of a dynamical system can have multifractal properties, i.e., demonstrate different local scaling. We try to find how the interaction of oscillatory systems affects the multifractal properties of the chaotic dynamics.

As an example, we choose the model of two coupled Rössler systems:

$$\begin{aligned}
\frac{\mathrm{d}x_{1,2}}{\mathrm{d}t} &= -\omega_{1,2}\, y_{1,2} - z_{1,2} + \gamma\,(x_{2,1} - x_{1,2})\,,\\
\frac{\mathrm{d}y_{1,2}}{\mathrm{d}t} &= \omega_{1,2}\, x_{1,2} + A y_{1,2}\,,\\
\frac{\mathrm{d}z_{1,2}}{\mathrm{d}t} &= B + z_{1,2}(x_{1,2} - \mu)\,,
\end{aligned} \tag{35}$$

where parameters A, B, and μ determine the dynamics of each system, γ is the coupling parameter, $\omega_1 = \omega_0 + \delta$ and $\omega_2 = \omega_0 - \delta$ are basic frequencies, and δ is the detuning. The calculations were performed for the following values of these parameters: $A = 0.15$, $B = 0.2$, $\gamma = 0.02$, $\mu = 6.8$, and $\omega_0 = 1.0$ [67].

System (35) demonstrates various coexisting synchronized regimes of chaotic oscillations and various types of asynchronous dynamics with different multifractal characteristics [26, 28]. We restrict our consideration to the case of transition over the boundary of the phase synchronization region with an increase in the parameter δ. The projections of the phase portraits of the system on the plane (x_1, x_2) for the synchronous and asynchronous chaos regimes are visually distinct (Fig. 10). We select the secant surface (for example, $x_2 = 0$) and analyze the shape of the singularity spectra $D(h)$ calculated using the sequence of recurrence times to this plane for the oscillations shown in Fig. 10.

As can be seen from Fig. 11, the function $D(h)$ is much wider in an asynchronous regime than in a synchronous regime (where the singularity spectrum collapses to a point). This means that the phase synchronization of chaotic oscillations in model (35) is accompanied by a loss of multifractality in the dynamics of the recurrence times. The asynchronous chaos regime shows a complex multifractal structure and is described by a wide spectrum of Hölder exponents (Fig. 11b). But for the synchronous case, the sequence of recurrence times to the secant plane can be regarded as a map of a process characterized by a value of $h(q)$ that is constant within the margin of error.

The width of the singularity spectrum can vary for different synchronous regimes. The most typical situation is where the sequence of recurrence times cannot be described by a constant value of $h(q)$. Moreover, calculating Hölder exponents at large values of q shows significant sensitivity to the choice of the counting parameters, for example, the range of the $\tau(q)$ approximation. It is therefore reasonable to introduce the characteristic of the multifractality degree Δ_h (the width of the singularity spectrum). The analysis of the various states of chaotic oscillations in system (35) shows that for any type of synchronous dynamics, the multifractality degree is much smaller than outside the synchronization domain [68]. Another difference from the singularity spectra shown in Fig. 11a is an increase in $h(q)$ for the asynchronous oscillations, which signifies a change in the type of correlations. The characteristics computed within the WTMM framework clearly show the transition boundary from the asynchronous regime to the synchronous (Fig. 12). We note that the transition from the synchronous regime can be diagnosed using other methods, but multifractal analysis yields a different perspective in considering this phenomenon: the chaos synchronization can be considered an effect due to transition from complex multifractal dynamics with a wide spectrum of Hölder exponents to simpler monofractal dynamics that can be quantitatively described by a single scaling exponent. The loss of multifractality signifies the leveling of various irregularities and a transition from a process containing several types of singular behavior to uniform (simpler) dynamics exhibiting only one type of singularity. The effects of the decrease in (loss of) multifractality with the chaotic synchronization are also observed in the dynamics of more complex models, considered, e.g., in [26].

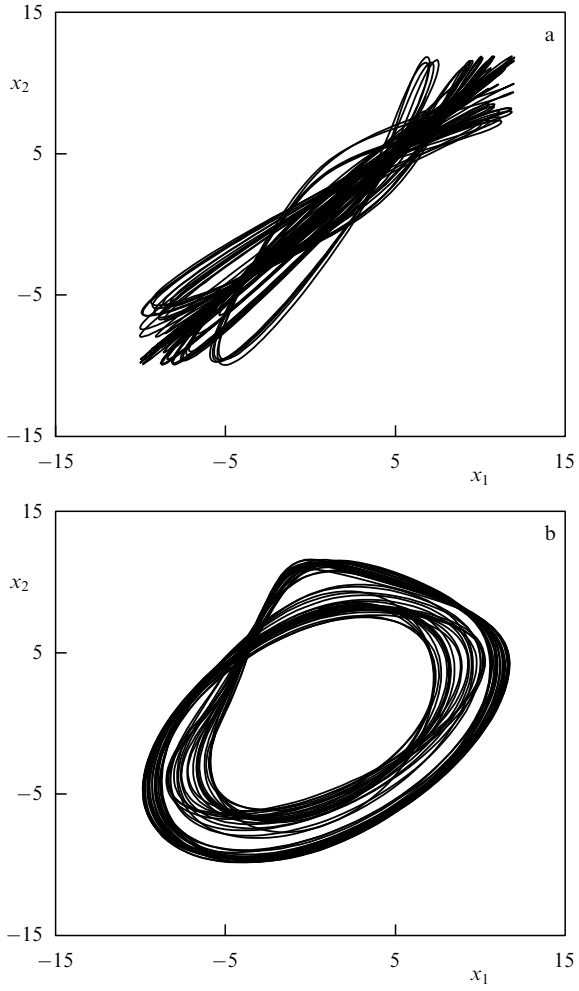

Figure 10. Synchronous (a) and asynchronous (b) chaos in the model of two coupled Rössler systems.

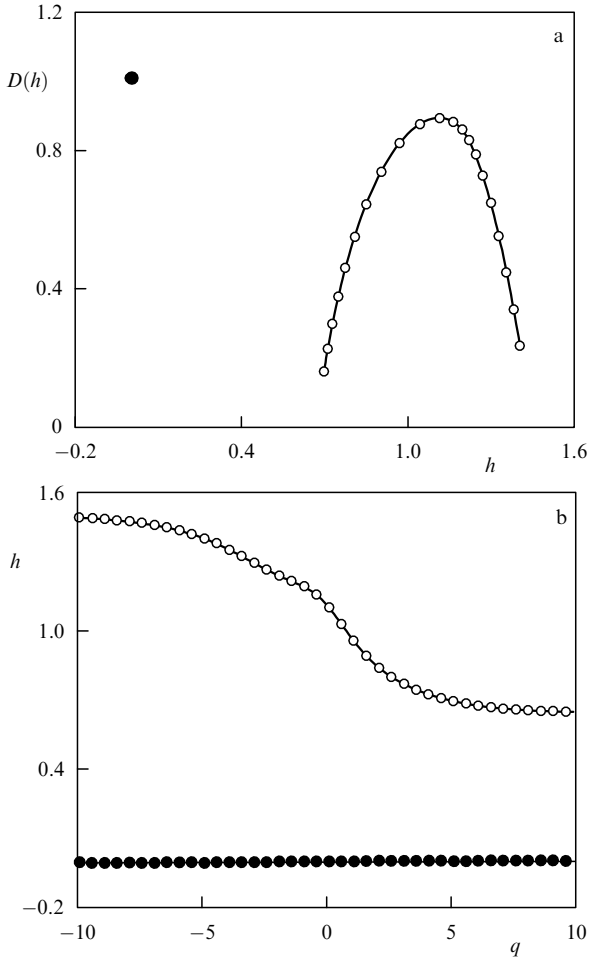

Figure 11. The singularity spectra (a) and $h(q)$ values (b) for synchronous (black circles) and asynchronous (white circles) chaotic regimes.

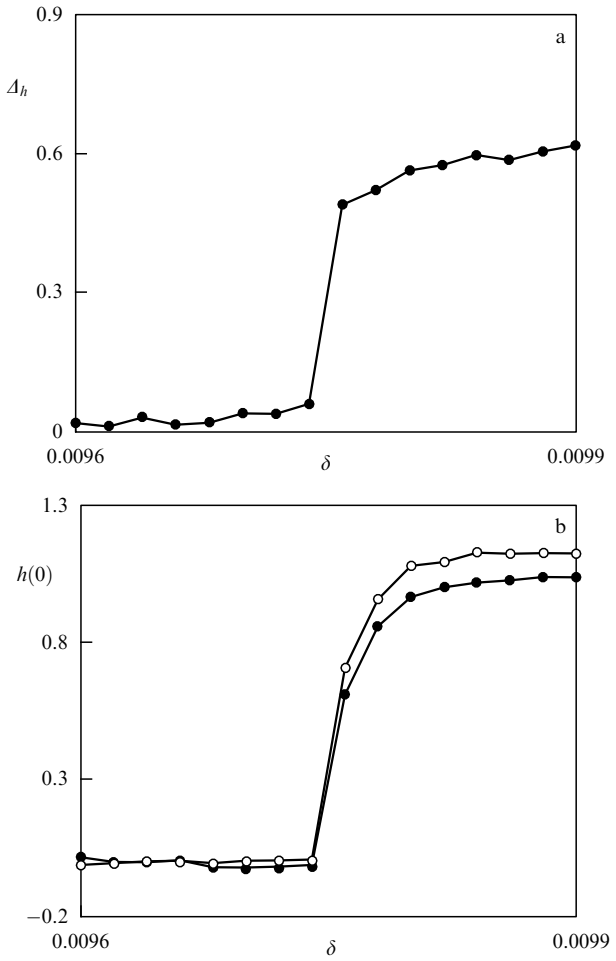

Figure 12. Transition through the boundary of the synchronization region, diagnosed by the characteristic changes in the multifractal formalism. Figure (b) shows the results of an analysis of the sequence of recurrence times separately for each of the two interacting systems (secant planes $x = 0$ and $x = 1$).

4.2 Stochastic synchronization

To illustrate the general tendency in the multifractal description of chaos synchronization effects and noise-induced ordering in nonlinear systems, we consider the well-known stochastic resonance effect [69–71].

Recently, the authors of [72] attempted to give a multifractal description of this effect for the model of an overdamped bistable oscillator described by the stochastic differential equation

$$\frac{\mathrm{d}x}{\mathrm{d}t} = x - x^3 + I\xi(t) + A\sin(\Omega t + \phi)\,, \tag{36}$$

where $\xi(t)$ is a normally distributed δ-correlated process (white noise), I the noise intensity, and A the amplitude of an external periodic force, which is a small value. Without noise, the system does not exhibit transitions between two states. In the study of a stochastic resonance, two cases are often considered, where the amplitude A of a periodic signal is very small compared to the potential barrier and where A is comparable to the barrier. In the second case, the dynamics of the bistable system show a large degree of coherency between the switching process and the input signal, which can be described using stochastic synchronization [73, 74]. According to the conclusion in [72], confirmed by our calculations, for a sufficiently large amplitude of the periodic signal, the effect of stochastic resonance is accompanied by the loss of multifractality in the dynamics of model (36). Changes in the parameter I significantly affect the structure of the singularity spectrum: at the optimum level of noise, corresponding to the resonance, the sequence of recurrence times to one of the bistable states has a clear monofractal structure (Fig. 13), but when moving away from this value, the singularity spectrum corresponds to a multifractal object. Thus, the stochastic synchronization regime is accompanied by the loss of multifractality in the dynamics of the overdamped bistable oscillator with an external force. This resembles chaos synchronization in the multifractal description discussed in Section 4.1.

4.3 Multifractal analysis of blood pressure dynamics

We consider a much more complicated case, the dynamics of living systems. It is known that many signals of biological origin are strongly nonuniform and nonstationary, and the most universal methods (whose efficiency does not depend on the stationarity of the processes) should be used for analysis. The multifractal wavelet transform method is one such universal method, as was shown, in particular in the paper by Ivanov et al. published in *Nature* [43]. Using the WTMM method, the authors demonstrated that physiological signals belong to the class of multifractal processes. In particular, the multifractal properties of the heartbeat for

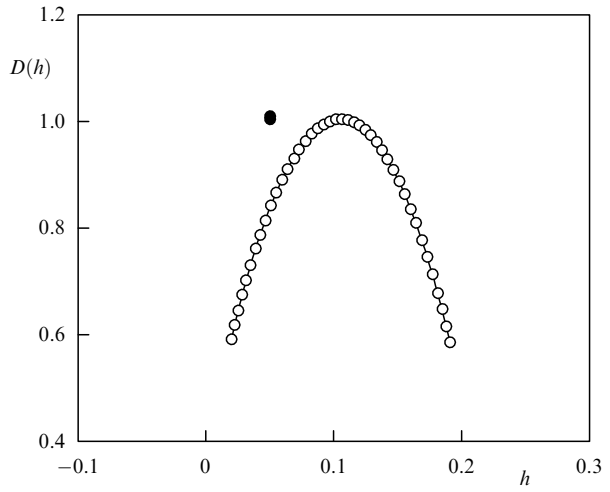

Figure 13. The singularity spectra corresponding to a stochastic synchronization switchover in a bistable system (black circle) and dynamics outside the synchronization domain (white circles).

healthy organisms differ from multifractal properties in the case of a pathology. In particular, the scaling characteristics of the WTMM method are possible diagnostic tools in biological systems [46, 47]. This is particularly important in the cases where the standard methods of signal structure analysis do not provide acceptable diagnostics (for example, in processing strongly nonstationary short-time processes).

Various external influences on the organism also change the characteristics of the multifractal structure of the heartbeat. In this section, as an illustration, we present the results of a multifractal description of the adaptation of the cardiac system to stress factors [75].

Experiments were conducted on 23 white rats (11 male and 12 female) with implanted intra-arterial catheters for direct measurements of blood pressure. The blood pressure was recorded at rest and under stress (by restricting the animal's motion). In preliminary processing, the initial data (Fig. 14a) were converted into point processes given by the sequences of time intervals between the local maxima of the arterial blood pressure signal (Fig. 14b). Then, these sequences were analyzed to detect stress-induced changes in the multifractal signal structure.

Two types of responses were found: stress leads to a significant decrease in the Hölder exponent (which implies changes in the local regularity and correlation property of the signals) (Fig. 15a) or to a decrease in the width of the singularity spectrum Δ_h (Fig. 15b). The last response is most interesting: due to stress, a multifractal process (the rat's

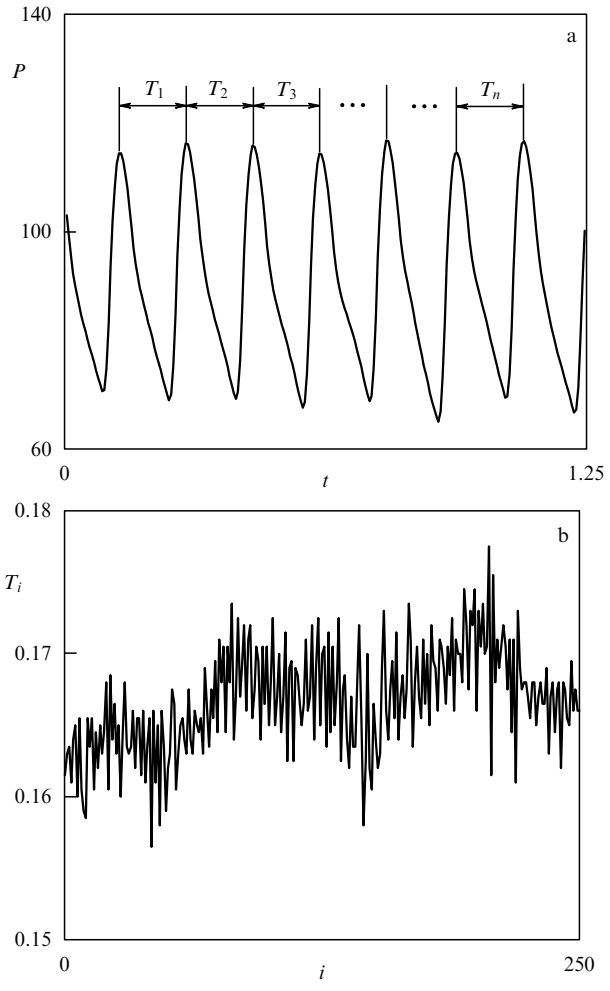

Figure 14. Signal of white rat's arterial blood pressure (a) and the extracted sequence of time intervals between local maxima of the signal (b).

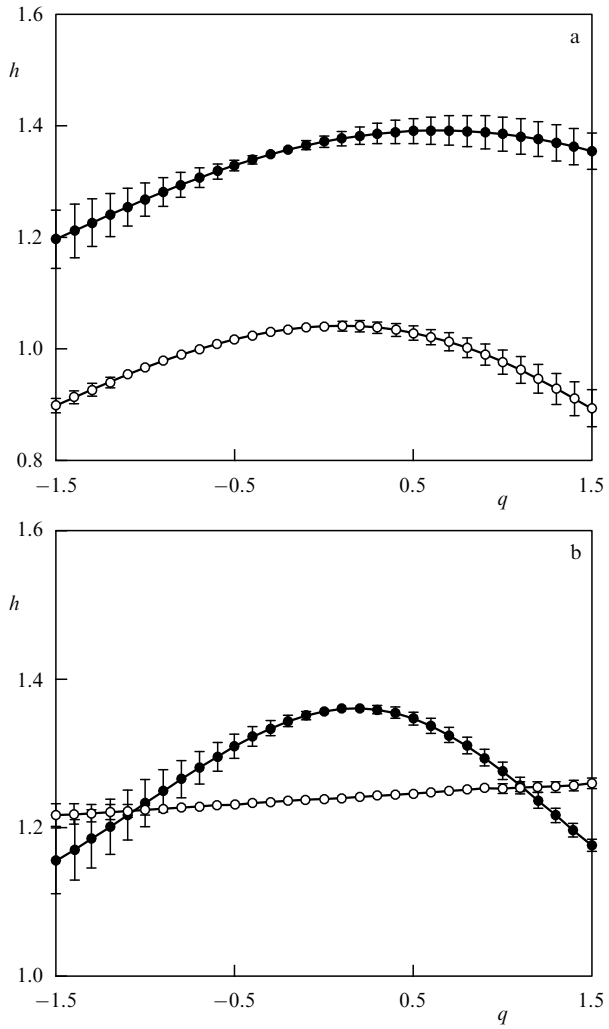

Figure 15. The response to stress causes changes in local regularity of the signal (correlation properties) (a) and loss of multifractality (b).

blood pressure in the normal state) becomes monofractal. Thus, the results of stress on the body in some cases can be based on the analysis of transition from a monofractal structure to a multifractal structure and vice versa. We note an important circumstance: standard analysis methods such as computing the heart-beat frequency or the spectral analysis, do not distinguish between the two types of response shown in Fig. 15. In both cases, similar changes were detected: an increase in the heart-beat frequency and energy characteristics. This example demonstrates a case where multifractal analysis can be an efficient method for classifying the state of a biological system based on short nonstationary signals.

In the study, clear distinctions between male and female rat responses were found. The blood pressure dynamics of the females show a weak response to stress (Fig. 16a), while the male dynamics show a much stronger change in the singularity spectrum $D(h)$ compared to the singularity spectrum at rest (Fig. 16b). The results in Fig. 16 are the most distinct, but very typical responses. As can be seen from Fig. 16b, the Hölder exponent $h(q)$ of a male's blood pressure signal decreases with stress, which signifies changes in correlation; the process becomes less smooth. In addition to changes in correlation, the value Δ_h also decreases. In the current example, $\Delta_h \approx 0.5$ at rest and $\Delta_h \approx 0.3$ during stress, i.e, the singularity spectrum becomes narrower. A significant decrease in Δ_h was detected in males in 7 experiments out of 11 and in 3 cases a transition to an almost monofractal structure of the point processes was observed. Because the rats were only weakly stressed, it is possible that a stronger influence would cause the loss of multifractalily more often. This suggests the hypothesis that the multifractal measure Δ_h can serve as an indicator of the strength of the organism's response to stress.

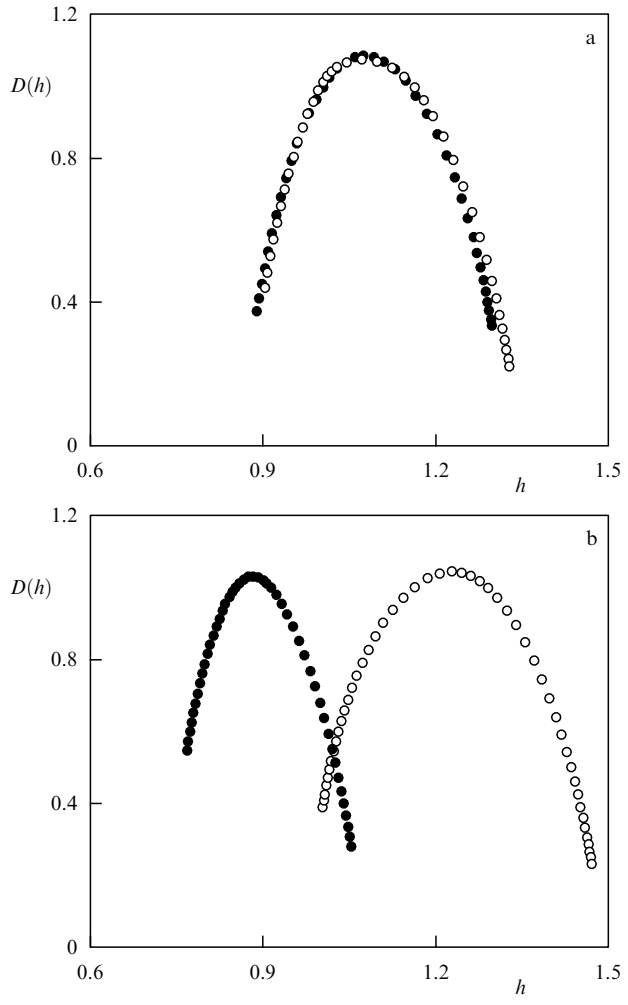

Figure 16. The typical response to stress for a female (a) and a male (b).

5. Capabilities and limitations of the multifractal analysis

The multifractal analysis on the wavelet transform based can be considered a method of study of spectral-correlation properties of various processes, including nonstationary ones. As follows, in particular, from Eqn (23), slow nonstationarity (a polynomial trend) does not affect the result if the selected basis function ψ is such that its first several moments vanish. Besides the possibility to study both stationary and nonstationary processes, the WTMM method has another advantage over the classical correlation analysis: being an instrument of a 'local' study of the structure of functions of time, the multifractal analysis allows estimating the correlation properties of random processes based on comparatively short signals. To illustrate the efficiency of WTMM usage for correlation signal analysis, we consider a Wiener random process, whose statistical properties are well known ($h = 1.5$).

The results of the classical correlation analysis show that for relatively short realizations of the same process, the estimates of the correlation decay can differ significantly. The rate of decay for different autocorrelation functions (Fig. 17) for different samples containing 3000 points differ by almost 2 times. The WTMM method shows the existence of a Wiener process based on the same sampling much more reliably. Assuming a homogeneous process, we can estimate the Hölder exponents averaged over q. These estimates give the expected value $h = 1.5$ with an error not exceeding 3%. The spread of characteristics for the decay rate in the autocorrelation function is much larger.

As another example, we consider white noise ($h = 0.5$) or $1/f$ noise ($h = 1$) and obtain the expected value of the Hölder exponent with an accuracy of the same order of magnitude ($\sim 3\%$ for a sample with 3000 points). But these examples deal with only very simple objects. To evaluate real capabilities and limitations of the multifractal method, one should consider a more complicated problem and analyze inhomogeneous signals containing various types of singular behavior.

In considering the simultaneous activity of several processes with different statistical properties and amplitudes, we can expect one of the processes to be present on a small scale (with weak singularities) and another on a large scale (strong singularities). For clarity, we consider an artificial signal that is a sum of a Wiener random process and a sequence of pulses with a Cantor set structure. It is expected that as a result of such summation (Fig. 18), the Cantor set structure is to be exhibited through large fluctuations and the Wiener random process is to dominate at small scales. The computations confirm this expectation (Fig. 19). The Hölder exponent approaches $h = 1.5$ at negative q (weak singularities) and $h \approx 0.63$ at positive q (strong singularities). Thus, the WTMM method clearly determines the differences in structure of the analyzed signal with changes in the scale of observations. In the case of several

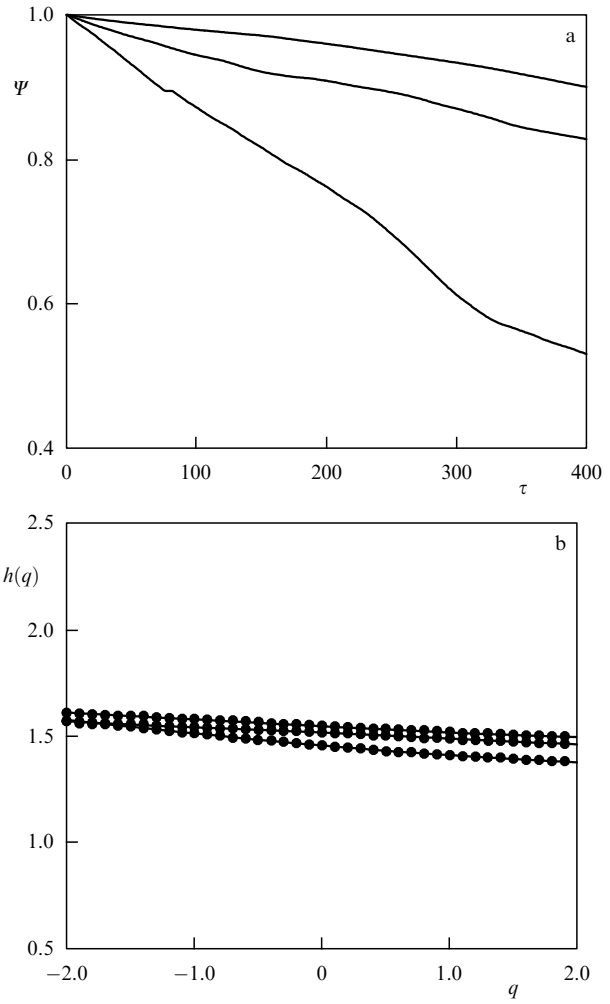

Figure 17. Results of computing the autocorrelation function (a) and the Hölder exponent (b) for three realizations of a random process containing 3000 points.

types of singularities, the WTMM method determines when these singularities belong to different scales. If the difference in scales is insignificant, then there is no clear separation of

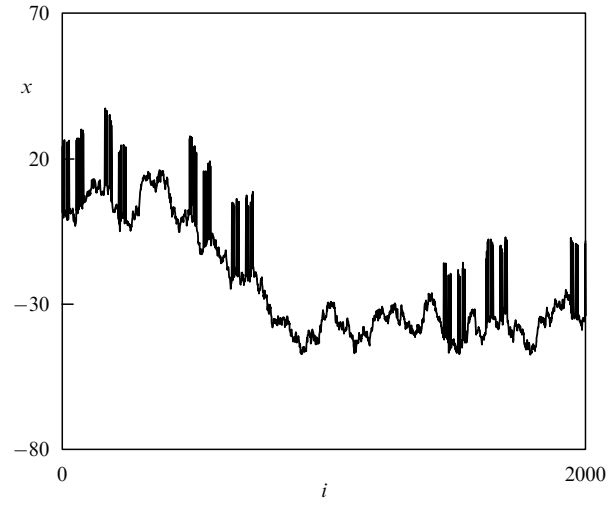

Figure 18. An artificial signal that is a sum of realizations of the Wiener random process and a sequence of pulses with the Cantor set structure.

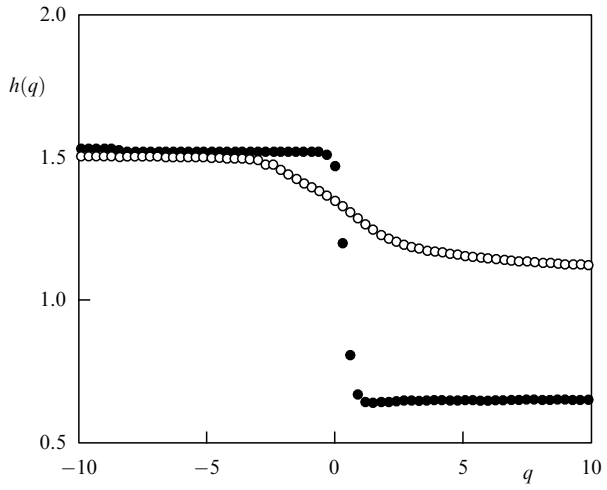

Figure 19. The $h(q)$ dependence for the signal shown in Fig. 18 (black circles). White circles correspond to the case of small differences in scales of observed singularities.

singularities. In particular, in the example considered with a sum of pulses of the Cantor set and the Wiener process, the increase in the intensity of the latter leads to shifting the Hölder exponent at $q > 0$ towards $h = 1.5$ (see Fig. 19). The second type of singularity ($h \approx 0.63$) can appear only at large q, but as q increases, the reliability of the estimates of Hölder exponents decreases. In the case of several types of singularities with similar scales, the WTMM method leads to averaged values of h.

The WTMM method may entail difficulties in the case of a special frequency-modulated behavior, observed for so-called chirps [76]. Alternating oscillatory functions are better studied using a more general approach, based on the double microlocal analysis proposed in [76]. The case of chirps shows the limitations of the WTMM method. Thus, this method is not applicable to the study of singular oscillatory functions. Another limitation of the multifractal analysis is that it only estimates the upper envelope of the true multifractal spectrum. This can lead to mistakes in interpreting the results. First, if the true singularity spectrum $D(h)$ is discrete, i.e., h takes only discrete values, then the envelope curve includes 'false' points that interpolate these discrete values. Second, the envelope does not identify the internal points (if they exist) that do not belong to the upper envelope of the spectrum $D(h)$ (Fig. 20). The authors of [77] point out that the bell-like shape of the singularity spectrum can be obtained even in the cases where the WTMM method is used to process signals without multifractal properties. If a process is characterized not by a continuous spectrum $D(h)$ but by a small set of Hölder exponents, then obtaining an envelope like that shown in Fig. 20 does not allow asserting in general whether there exist singularities, for example, characterized by $h = 0.63 \pm 0.005$. To avoid difficulties in interpreting the results, it is better not to attempt to determine whether the number of scaling characteristics a is finite or infinite but to consider the WTMM method as a numerical tool for estimating the range of the Hölder exponent (i.e., the multifractality degree) and determining the existence and characterization of various types of correlations in nonstationary random processes. We thus have an opportunity to perform a correlation analysis of short-time nonstationary signals and

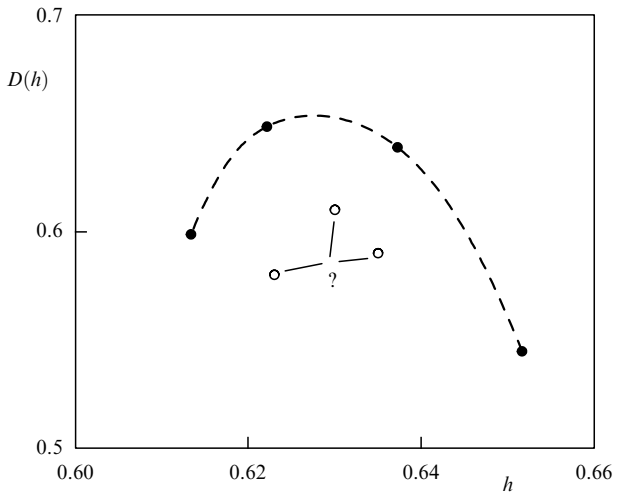

Figure 20. An illustration of the limitations of the multifractal formalism methods. Black circles correspond to the actual multifractal spectrum, the dashed line represents the results of multifractal analysis. The internal points (white circles) cannot be identified using the WTMM method.

numerically evaluate the inhomogeneity degree of a random process.

6. Conclusions

The existence of multifractality or complex scaling in the structure of various natural processes has been widely discussed in the scientific literature in recent years. The appearance of a new tool for complex signal analysis, based on a combination of multifractal theory and wavelet analysis, significantly increases the ability to use rigorous mathematical results in experimental studies.

Multifractal analysis based on the continuous wavelet transform can be interpreted as a novel look at the problem of signal structure analysis. In statistical radio-physics problems, in particular, considerable attention is traditionally given to spectrum-correlation analysis. But classical methods of calculating correlation functions or power spectra can be used only for stationary processes, and long-time signals are required to obtain reliable estimates of correlation decay or of the frequency dependence of the spectral density function. In contrast to the classical approaches, the WTMM method allows performing correlation analysis using rather short and nonstationary signals, which positions this method as a tool for studying the structure of real processes obtained in experiments. Moreover, this tool is quite universal and can be applied independently of the stationarity and the nature of the signal: processes obtained from physical experiments, biomedical studies, and meteorological series can all be successfully analyzed.

Multifractal analysis presents an interesting tool for studying the dynamics of living systems. These systems often exhibit complex irregular behavior whose characteristics constantly change with time. Using classical probability and spectral methods for such analysis means making an a priori assumption that these processes are approximately ergodic, but the veracity of such assumptions is difficult to justify when a living organism constantly adapts to changing environmental conditions. Problems often arise in interpreting analyses of biological data. For example, the existence of two peaks in a power spectrum whose frequencies are not a multiple of one another can correspond to two opposite situations: the dynamics of the studied system can contain two independent rhythms, or the frequency is changing and only one rhythmical process is detected at each instant. These situations, which often arise in functions of living natural objects, demonstrate the restrictions of classical methods for analyzing these random processes and point to the necessity of using more efficient tools of signal analysis. Modern biological studies are impossible without applying special physical methods. The development of modern equipment led to advanced experimental studies where biological signals can be measured on a microscopic scale of separate cells and intracellular dynamics. But the analysis of these signals is often reduced to simple statistical processing of experimental data. Introducing more precise instruments for signal structure analysis, which detect complex structures, is becoming an urgent problem: modern high-precision biological experiments clearly need the corresponding analysis methods. Applying methods from physics to problems in biology undoubtedly enriches physics itself. In particular, developing special methods not restricted by nonstationarity not only significantly increases the opportunity of experimental studies but also determines future progress in the evolution of signal structure analysis. Along with the well-known wavelet analysis, the multifractal method based on the wavelet transform can justifiably assume this role.

Acknowledgments. We are grateful to all our colleagues who collaborated with us during the study of these problems. We are particularly grateful to O V Ivanov for his attention to this work and a number of valuable suggestions. We are thankful to the Science and Education Ministry of the Russian Federation for the support within the Development of Scientific Potential in Universities (2006 – 2008) program.

References

1. Mandelbrot B B *The Fractal Geometry of Nature* (San Francisco: W.H. Freeman, 1982)
2. Halsey T C et al. *Phys. Rev. A* **33** 1141 (1986)
3. Tel T *Z. Naturforsh. A* **43** 1154 (1988)
4. Feder J *Fractals* (New York: Plenum Press, 1988) [Translated into Russian (Moscow: Mir, 1991)]
5. Schroeder M *Fractals, Chaos, Power Laws*: *Minutes from an Infinite Pardise* (New York: W.H. Frecman, 1991) [Translated into Russian (Moscow Izhevsk: RKhD, 2001)]
6. Paitgen H-O, Richter P H *The Beauty of Fractals* (Berlin: Springer-Verlag, 1986) [Translated into Russian (Moscow: Mir, 1993)]
7. Family F, Vicsek T *Dynamics of Fractal Surfaces* (Singapore: World Scientific, 1991)
8. Zel'dovich Ya B, Sokolov D D *Usp. Fiz. Naik* **146** 493 (1985) [*Sov. Phys. Usp.* **28** 608 (1985)]
9. Sokolov I M *Usp. Fiz. Naik* **150** 221 (1986) [*Sov. Phys. Usp.* **29** 924 (1986)]
10. Zosimov V V, Lyamshev L M *Usp. Fiz. Nauk* **165** 361 (1995) [*Phys. Usp.* **38** 347 (1995)]
11. Vainshtein S I et al. *Phys. Rev. E* **50** 1823 (1994)
12. Eisenberg E et al. *Phys. Rev. E* **47** 2333 (1993)
13. Dräger J, Bunde A *Phys. Rev. E* **54** 4596 (1996)
14. Arneodo A, Decoster N, Roux S G *Phys. Rev. Lett.* **83** 1255 (1999)
15. Chhabra A B et al. *Phys. Rev. A* **40** 5284 (1989)
16. Benzi R et al. *J. Phys. A*: *Math. Gen.* **17** 3521 (1984)
17. Badii R, Broggi G *Phys. Lett. A* **131** 339 (1988)
18. Feigenbaum M J *J. Stat. Phys.* **46** 919 (1987)
19. Jensen M H, Kadanoff L P, Procaccia I *Phys. Rev. A* **36** 1409 (1987)
20. Mandelbrot B B *Fractals and Multifractals*: *Noise, Turbulence and Galaxies* (New York: Springer – Verlag, 1989)
21. Strait B J, Dewey T G *Phys. Rev. E* **52** 6588 (1995)

22. Glazier J A et al. *Phys. Rev. E* **51** 2665 (1995)
23. Hentschel H G E *Phys. Rev. E* **50** 243 (1994)
24. Wiklund K O, Elgin J N *Phys. Rev. E* **54** 1111 (1996)
25. Pavlov A N et al. *Physica A* **300** 310 (2001)
26. Pavlov A N et al. *Physica A* **316** 233 (2002)
27. Frish U, Parisi G, in *Turbulence and Predictability in Geophysical Fluid Dynamics and Climate Dynamics* (Proc. of the Intern. School of Physics "Enrico Fermi", Course 88, Eds M Ghil, R Benzi, G Parisi) (Amsterdam: North-Holland, 1985) p. 71
28. Barabási A-L, Vicsek T *Phys. Rev. A* **44** 2730 (1991)
29. Gagne Y, Hopfinger E, Frisch U, in *New Trends in Nonlinear Dynamics and Pattern-Forming Phenomena: The Geometry of Nonequilibrium* (NATO ASI Series. Ser. B, Vol. 237, Eds P Coullet, P Huerre) (New York: Plenum Press, 1990) p. 315
30. Muzy J F, Bacry E, Arneodo A *Phys. Rev. Lett.* **67** 3515 (1991)
31. Muzy J F, Bacry E, Arneodo A *Phys. Rev. E* **47** 875 (1993)
32. Grossmann A, Morlet J *SIAM J. Math. Anal.* **15** 723 (1984)
33. Meyer Y *Wavelets: Algorithms and Applications* (Philadelpha, Pa.: Society for Industrial and Applied Mathematics, 1993)
34. Meyer Y *Wavelets and Operators* (Cambridge: Cambridge Univ. Press, 1992)
35. Daubechies I *Ten Lectures on Wavelets* (Philadelpha, Pa.: Society for Industrial and Applied Mathematics, 1992)
36. Chui C K *An Introduction to Wavelets* (Boston: Academic Press, 1992)
37. Mallat S *A Wavelet Tour of Signal Processing* (San Diego: Academic Press, 1998)
38. Astaf'eva N M *Usp. Fiz. Nauk* **166** 1145 (1996) [*Phys. Usp.* **39** 1085 (1996)]
39. Dremin I M, Ivanov O V, Nechitaĭlo V A *Usp. Fiz. Nauk* **171** 465 (2001) [*Phys. Usp.* **44** 447 (2001)]
40. Koronovskii A A, Khramov A E *Nepreryvnyi Veivletnyi Analiz i Ego Prilozheniya* (Continuous Wavelet Analysis and Its Applications) (Moscow: Fizmatlit, 2003)
41. Sosnovtseva O V et al. *Phys. Rev. Lett.* **94** 218103 (2005)
42. Pavlov A N et al. *Brief. Bioinform.* **7** 375 (2006)
43. Ivanov P Ch et al. *Nature* **399** 461 (1999)
44. Arneodo A et al. *Physica A* **249** 439 (1998)
45. Stanley H E et al. *Physica A* **270** 309 (1999)
46. Nunes Amaral L A et al. *Phys. Rev. Lett.* **86** 6026 (2001)
47. Ivanov P Ch et al. *Chaos* **11** 641 (2001)
48. Marrone A et al. *Phys. Rev. E* **60** 1088 (1999)
49. Thurner S, Feurstein M C, Teich M C *Phys. Rev. Lett.* **80** 1544 (1998)
50. Gabor D *J. IEE* (London) **93** 429 (1946)
51. Vainshtein L A, Vakman D E *Razdelenie Chastot v Teorii Kolebanii i Voln* (Moscow: Nauka, 1983)]
52. Peng C-K et al. *Chaos* **5** 82 (1995)
53. Peng C-K et al. *Phys. Rev. E* **49** 1685 (1994)
54. Hausdorff F *Math. Ann.* **79** 157 (1918)
55. Besicovitch A S *Math. Ann.* **110** 321 (1935)
56. Falconer K J *The Geometry of Fractal Sets* (Cambridge: Cambridge Univ. Press, 1985)
57. Farmer J D, Ott E, Yorke J A *Physica D* **7** 153 (1983)
58. Muzy J F, Bacry E, Arneodo A *Int. J. Bifurcat. Chaos* **4** 245 (1994)
59. Bozhokin S V, Parshin D A *Fraktaly i Mul'tifraktaly* (Moscow – Izhevsk: RKhD, 2001)
60. Grassberger P *Phys. Lett. A* **97** 227 (1983)
61. Grassberger P, Procaccia I *Physica D* **9** 189 (1983)
62. Hentschel H G E, Procaccia I *Physica D* **8** 435 (1983)
63. Grassberger P, Procaccia I *Phys. Rev. Lett.* **50** 346 (1983)
64. Bowen R *Equilibrium States and the Ergodic Theory of Anosov Diffeomorphisms* (Lecture Notes in Mathematics, Vol. 470) (Berlin: Springer-Verlag, 1975)
65. Collet P, Lebowiz J L, Porzio A *J. Stat. Phys.* **47** 609 (1987)
66. Afraimovich V, Zaslavsky G M *Phys. Rev. E* **55** 5418 (1997)
67. Postnov D E et al. *Chaos* **9** 227 (1999)
68. Pavlov A N, Sosnovtseva O V, Mosekilde E *Chaos, Solitons Fractals* **16** 801 (2003)
69. Benzi R, Sutera A, Vulpiani A *J. Phys. A: Math. Gen.* **14** L453 (1981)
70. Nicolis C, Nicolis G *Tellus* **33** 225 (1981)
71. Anishchenko V S et al. *Usp. Fiz. Nauk* **169** 7 (1999) [*Phys. Usp.* **42** 7 (1999)]
72. Silchenko A, Hu C-K *Phys. Rev. E* **63** 041105 (2001)
73. Anishchenko V S et al. *Nonlinear Dynamics of Chaotic and Stochastic Systems* (Berlin: Springer, 2002)
74. Anishchenko V S et al. *Nelineinye Effekty v Khaoticheskikh i Stokhasticheskikh Sistemakh* (Moscow – Izhevsk: Inst. Komp. Issled., 2003); see *also Nonlinear Dynamics of Chaotic and Stochastic Systems* 2nd ed. (Berlin: Springer, 2007)
75. Pavlov A N, Ziganshin A R, Klimova O A *Chaos, Solitons Fractals* **24** 57 (2005)
76. Jaffard S, Meyer Y *Mem. Am. Math. Soc.* **123** 587 (1996)
77. Veneziano D, Moglen G E, Bras R L *Phys. Rev. E* **52** 1387 (1995)